Optics Letters

Photonic gauge potential in a system with a synthetic frequency dimension

LUQI YUAN, YU SHI, AND SHANHUI FAN*

Department of Electrical Engineering, and Ginzton Laboratory, Stanford University, Stanford, California 94305, USA
**Corresponding authors: shanhui@stanford.edu*

Received 16 November 2015; accepted 2 January 2016; posted 6 January 2016 (Doc. ID 253982); published 5 February 2016

We generalize the concept of photonic gauge potential in real space by introducing an additional "synthetic" frequency dimension in addition to the real space dimensions. As an illustration, we consider a one-dimensional array of ring resonators, each supporting a set of resonant modes having a frequency comb with spacing Ω, and undergoing a refractive index modulation at the modulation frequency equal to Ω. We show that the modulation phase provides a gauge potential in the synthetic two-dimensional space with the dimensions being the frequency and the spatial axes. Such a gauge potential can create a topologically protected one-way edge state in the synthetic space that is useful for high-efficiency generation of higher-order side bands.

OCIS codes: (060.2630) Frequency modulation; (230.5750) Resonators; (230.7405) Wavelength conversion devices.

http://dx.doi.org/10.1364/OL.41.000741

The creation of photonic gauge potential in real space opens a new dimension in the control of light propagation. Such real-space photonic gauge potential can be created either in time-reversal invariant systems, such as a static resonator lattice or metamaterials [1–3], or in systems where time-reversal symmetry is broken with either magneto-optical [4] or dynamic modulation effects [5]. Similar concepts of a gauge potential can be achieved in the acoustic systems [6]. A proper choice of photonic gauge potential can lead to an effective magnetic field for photons [1,5,7], which directly results in the creation of topologically protected one-way edge states. The ability to specify arbitrary gauge potential in real space, moreover, can lead to novel effects, including negative refraction [8], directional-dependent total internal reflection [8], and gauge-field waveguides [9]. The concept of photonic gauge potential in real space is also intimately connected to the concept of photonic gauge potential in momentum space [10–15], both of which are of significant importance in the emerging area of topological photonics [16–20].

In this Letter we generalize the concept of the photonic gauge potential in real space by adding a "synthetic" frequency dimension to the real space dimensions. As an illustration, we start by considering a simple one-dimensional coupled resonator model shown in Fig. 1(a). Each resonator supports a set of modes with their frequencies equally spaced at a frequency Ω, forming a frequency comb. We assume coupling only between modes having the same frequency at the nearest neighbor resonators. In addition, we assume that each resonator is modulated at the frequency Ω, which induces coupling between modes in the same resonator with frequencies separated by Ω. The Hamiltonian of the system is then

$$H = \sum_{l,m} \omega_m a_{l,m}^\dagger a_{l,m} + \sum_{l,m} \{\kappa(a_{l,m}^\dagger a_{l+1,m} + a_{l+1,m}^\dagger a_{l,m}) + 2g\cos(\Omega t + \varphi_l)(a_{l,m}^\dagger a_{l,m+1} + a_{l,m+1}^\dagger a_{l,m})\}, \quad (1)$$

where $a_{l,m}^\dagger (a_{l,m})$ is the creation (annihilation) operator for the m-th mode at the l-th resonator; $\omega_m = \omega_0 + m\Omega$ gives the frequency for the m-th resonant mode, κ is the coupling constant between two nearest-neighbor resonators, g is the strength of modulation, and φ_l is the associated modulation phase at the l-th resonator. Below we will show that this Hamiltonian is equivalent to a tight-binding Hamiltonian in two dimensions subject to an out-of-plane effective magnetic field, with each lattice site corresponding to one mode in a specific resonator,

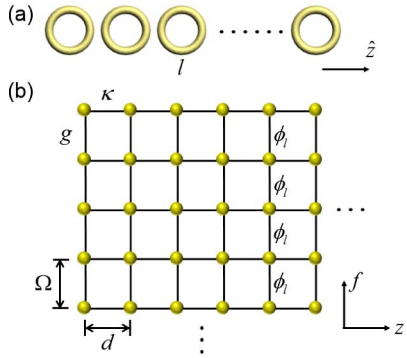

Fig. 1. (a) A one-dimensional array of ring resonators. Each ring resonator supports a set of resonant modes with the frequencies of the modes forming a frequency comb with equally spaced Ω. The l-th ring undergoes a modulation at the modulation frequency Ω with a modulation phase φ_l. (b) The system in the panel (a) can be mapped into a tight-binding model in two dimensions, with the extra synthetic dimension being the frequency dimension.

and with the two dimensions corresponding to the one-dimensional space and the frequency axes, respectively. In this construction the frequency axis therefore becomes an extra synthetic dimension.

The concept of synthetic dimension in the study of artificial gauge field has been recently discussed for cold atoms [21], where the synthetic dimension corresponds to the atomic states, and in a photonic system where the synthetic dimension corresponds to the orbital angular momentum of light [22]. In contrast to these works, here we show that the use of the frequency space as the synthetic dimension offers new possibilities for controlling the frequencies of light.

To see the emergence of an effective magnetic field in Eq. (1), we define $c_{j,m} \equiv a_{j,m}e^{-i\omega_m t}$, and apply the rotating wave approximation to obtain from Eq. (1)

$$H = \sum_{l,m}\{\kappa(c^{\dagger}_{l,m}c_{l+1,m} + c^{\dagger}_{l+1,m}c_{l,m}) + g(e^{-i\varphi_l}c^{\dagger}_{l,m}c_{l,m+1} + e^{i\varphi_l}c^{\dagger}_{l,m+1}c_{l,m})\}. \quad (2)$$

Equation (2) is identical in form to the Hamiltonian of a quantum particle on a two-dimensional lattice subject to a magnetic field [5], except that here, one of the axes (as labeled by the modal index m) is the frequency axis. Because there is one modulator per resonator, the hopping phases are uniform along the frequency axis. Nevertheless, Eq. (2) is sufficient to implement the Landau gauge for a uniform magnetic field by choosing

$$\varphi_l = l \cdot \pi/2. \quad (3)$$

The resulting system has the periodicity of $4d$ along the z-direction, where d is the physical spacing between the nearest neighbor resonators, and Ω along the frequency dimension. For an infinite lattice, we can re-write Eq. (2) into the $\boldsymbol{k}$-space

$$H_k = \sum_{\alpha=1}^{4}\{\kappa(a^{\dagger}_{k,\alpha}a_{k,\alpha+1}e^{ik_z d} + a^{\dagger}_{k,\alpha+1}a_{k,\alpha}e^{-ik_z d}) + 2g a^{\dagger}_{k,\alpha}a_{k,\alpha}\cos(k_f\Omega - \varphi_\alpha)\}, \quad (4)$$

where $\varphi_\alpha = \pi/2, \pi, 3\pi/2, 2\pi$, respectively. We plot the band structure, as defined as the eigenvalues of the Hamiltonian in (4) as a function of $\boldsymbol{k}$ in Fig. 2(a) with $g = \kappa$. There are 4 bands with Chern number −1, 1, 1, and −1, respectively. The band gaps between the top two bands and between the bottom two bands are therefore topologically nontrivial.

For a finite lattice, the nontrivial topology manifests in the creation of topologically protected one-way edge states in the eigenvalue ranges of the band gaps. As an illustration, we consider a system as described by the Hamiltonian of Eq. (2) with 21 resonators, assuming that the frequency axis is still infinite. The projected band structure, defined as the eigenvalues of Eq. (2) with respect to the wavevector k_f along the frequency axis, is shown in Fig. 2. We indeed observe two one-way edge states in the band gaps. Unlike the standard tight-binding models with two spatial dimensions, however, here the edge states corresponds to propagation in the *frequency* space. As a result the concept of a synthetic dimension of frequencies allows novel possibility for manipulating the frequency of light.

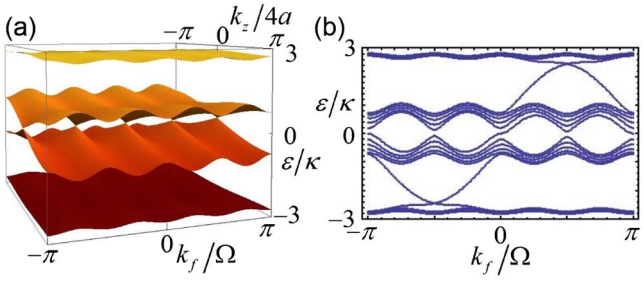

Fig. 2. (a) Band structure for the system shown in Fig. 1, as described by the Hamiltonian in Eq. (4) in the range $-\pi/4a < k_z < \pi/4a$ and $-\pi/\Omega < k_f < \pi/\Omega$. (b) Projected band structure for the system consisting of 21 resonators.

We now provide a physical system that implements the idea of synthetic dimension as described in Eq. (1). For this purpose we consider a one-dimensional array of optical ring resonators. Each ring resonator consists of a single-mode waveguide forming a loop. The waveguide has a dispersion relation

$$\beta = n(\omega)\frac{\omega}{c}, \quad (5)$$

where β is the wavevector along the propagation direction, which will be denoted as the x-direction. $n(\omega)$ is the effective phase index. For a ring with a circumference L, suppose it supports a resonance at ω_0, i.e., $\beta(\omega_0)L = 2\pi m_0$. In the vicinity of ω_0, the resonance condition is

$$[\beta(\omega'_m) - \beta(\omega_0)]L = 2\pi m, \quad (6)$$

where ω'_m is the resonant frequency of the m-th order mode. If one ignores group velocity dispersion, then

$$\omega'_m = \omega_m \equiv \omega_0 + m\Omega, \quad (7)$$

where $\Omega \equiv 2\pi c/Ln_g(\omega_0)$, with the group index $n_g(\omega_0) = n + \omega\frac{\partial n}{\partial\omega}|_{\omega_0}$, and m is an integer. Below we refer to the fields at ω_m as the m-th side band. On the other hand, with group velocity dispersion, i.e., when $\partial n_g/\partial\omega \neq 0$, ω'_m and ω_m are no longer the same.

Suppose we modulate the ring at the modulation frequency Ω. The electric field inside the ring in general can be written as

$$E(t, r_\perp, x) = \sum_m \mathcal{E}_m(t, x)E_m(r_\perp)e^{i\omega_m t}, \quad (8)$$

where $r_\perp$ denotes the directions perpendicular to the waveguide, and $E_m(r_\perp)$ is the modal profile of the waveguide. $\mathcal{E}_m(t, x)$ is the modal amplitude associated with the m-th sideband. Assuming that the modal amplitudes are slowly varying, we then have [23]

$$\left(\frac{\partial}{\partial x} + i\beta(\omega_m)\right)\mathcal{E}_m - \frac{n_g(\omega_m)}{c}\frac{\partial}{\partial t}\mathcal{E}_m = 0, \quad (9)$$

with $\mathcal{E}_m(t, x + L) = \mathcal{E}_m(t, x)$.

We describe the coupling of the fields between the l-th and $(l+1)$-th resonators as

$$\mathcal{E}^l_m(t^+, x^l_1) = \sqrt{1-\gamma^2}\mathcal{E}^l_m(t^-, x^l_1) - i\gamma\mathcal{E}^{l+1}_m(t^-, x^{l+1}_2), \quad (10)$$

$$\mathcal{E}^{l+1}_m(t^+, x^{l+1}_2) = \sqrt{1-\gamma^2}\mathcal{E}^{l+1}_m(t^-, x^{l+1}_2) - i\gamma\mathcal{E}^l_m(t^-, x^l_1), \quad (11)$$

where γ represents the coupling strength. x^l_1 and x^{l+1}_2 are the positions on the two rings where the coupling occurs [see Fig. 3(a)], and $t^{\pm} = t + 0^{\pm}$.

We assume that the dynamic modulation of the l-th ring is achieved by placing a phase modulator at x^l_0 [Fig. 3(a)]. Upon

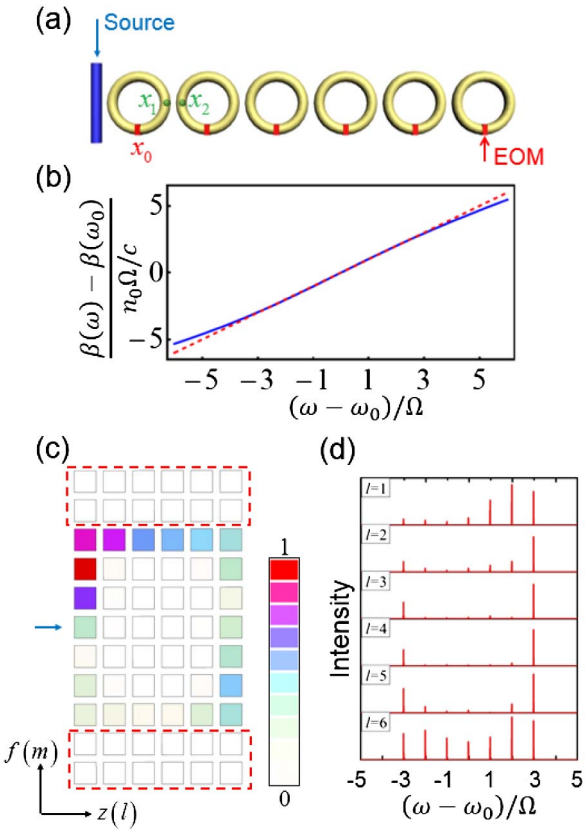

Fig. 3. (a) An array of six ring resonators. The red dots represent the electro-optic modulator (EOM) on the resonators. The green dots represent the positions where coupling occurs between the nearest neighbor resonators. An input waveguide couples to the left-most ring resonator. (b) The dispersion relation of the waveguide that forms the ring. (c) The distribution of the total intensity in each ring resonator for each frequency component ($|\mathcal{E}_{l,m}|^2$). The blue arrow indicates the continuous source. The frequency components in the dashed red box correspond to the non-resonant frequency sidebands. (d) The intensity spectra for the field $E(t, r)$ at each resonator.

passing through x_0^l, the total electric field undergoes a phase modulation $E \to Ee^{i\alpha \sin(\Omega t+\varphi)}$ [24], or equivalently

$$\mathcal{E}_m^l(t^+, x_0^l) = J_0(\alpha)\mathcal{E}_m^l(t^-, x_0^l) + \sum_q J_q(\alpha)\mathcal{E}_{m-q}^l(t^-, x_0^l)e^{iq\varphi} + \sum_q (-1)^q J_q(\alpha)\mathcal{E}_{m+q}^l(t^-, x_0^l)e^{-iq\varphi}, \quad (12)$$

where J_q is the Bessel function of the q-th order. The modulation therefore induces a coupling between sidebands, with the modulation phase appearing as the phase in the coupling constant, similar to the tight-binding model of Eqs. (1) and (2). Unlike the tight-binding model, here there is a long-range coupling in the frequency space. We will show in the simulation below that such a long-range coupling does not fundamentally affect the physics of synthetic dimension as described simply in the tight-binding model.

The excitation is injected into the system through an input/output waveguide

$$\mathcal{E}_m^l(t^+, x_e^l) = \sqrt{1-\eta^2}\mathcal{E}_m^l(t^-, x_e^l) - i\eta\mathcal{E}_s(t^-, x_e^l), \quad (13)$$

where η is the strength of the coupling between the resonator and the waveguide and $\mathcal{E}_s$ is the source field in the waveguide.

Equations (9)–(13) provide a description of a physical system consisting of a set of ring resonators coupled together, with each ring modulated by an electro-optic phase modulator. We solve Eq. (9) with a finite difference approach in both space and time. At the places where the coupling occurs or at the locations of the modulators, we calculate the fields at time t^- first with Eq. (9), and then apply either Eqs. (10) and (11) or Eq. (12) to compute the fields at t^+.

In the modulated ring, with the absence of group velocity dispersion, the modulation sidebands at ω_m coincide with the modes of the ring at ω_m'. Therefore we have on-resonance coupling between multiple modes. On the other hand, with group velocity dispersion, $\omega_m' \neq \omega_m$, and the coupling between the modes become off-resonance. As a result, the group velocity dispersion of a waveguide provides a natural "boundary" in the frequency space. As an illustration, we first perform a simulation of a system with six ring resonators as shown in Fig. 3(a). We assume that at a center frequency ω_0 the waveguide for the ring has an effective index of $n_0 = n(\omega_0) = 1.5$. In the simulation, we include 11 side bands ($\omega_m = \omega_0 + m\Omega$ and $m = -5, -4, \ldots, 5$), where $\Omega = 2\pi c/n_0 L$. We choose a waveguide dispersion relation $\beta(\omega)$, as shown in Fig. 3(b), such that 7 of the side bands with $m = -3, -2, \ldots, 3$ are on-resonance having $n(\omega_m) = n_0$. The other 4 side bands have an effective index that differs from n_0. The dispersion relation here thus is chosen to illustrate a waveguide with a zero group velocity dispersion near frequency ω_0. Each of the rings is modulated as described above with an electro-optic modulator with a modulation frequency Ω, and with a modulation phase φ_l in Eq. (3). To excite the system, a continuous-wave signal, having a single frequency at $\omega_{m=0}$, is sent into the left ring resonator ($l = 1$). The distribution of the intensity $|\mathcal{E}_{l,m}|^2$ as a function of l and m at $t = 400\ n_0 L/c$ (when the field finishes one loop in the synthetic space) is plotted in Fig. 3(c). We note that there is almost zero intensity for the sidebands with $m = \pm 5$ and ± 4. Thus the group velocity dispersion indeed provides a boundary in the frequency space. The intensity is concentrated at the edge of the synthetic space forming a topologically protected one-way mode. We plot in Fig. 3(d) the intensity spectra corresponding to the $E(t, r)$ field inside each resonator. For the resonators at the spatial edge, ($l = 1$, and $l = 6$), the intensity spectra have significant components in all on-resonance side bands, while for the resonators at the center of the structure ($l = 3$, and $l = 4$), the intensity spectra are almost completely concentrated in the on-resonance side bands that have the highest and lowest frequencies.

In a typical ring resonator system under modulation, multiple side bands are generated. On the other hand, in the system considered here the resonators in the center of the structure have amplitudes only in the highest and lowest on-resonance frequency side bands. Therefore, the use of a gauge field in the synthetic space provides the opportunity to create high-efficiency generation of high-order side-bands. As an illustration, we consider the system shown in Fig. 4(a). The system consists of five resonators modulated at a frequency Ω with the modulation phase chosen according to Eq. (3) such that we have a nonzero gauge field in the synthetic space. In the simulations, we include 11 side bands ($m = -5, \ldots + 5$). We choose the waveguide dispersion relation such that the side bands at

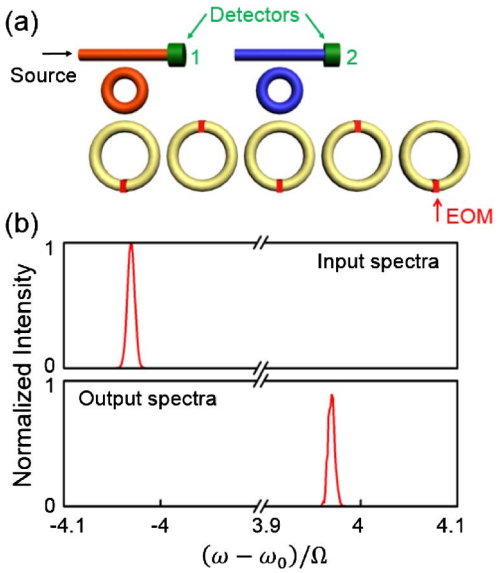

Fig. 4. (a) An array of five ring resonators. Two extra single-mode resonators couple between the array and the waveguides with detectors. (b) The intensity spectra of the input and output. The output spectra is measured at detector 2.

$m=\pm 5$ are non-resonant and the rest of the side bands are resonant with the ring modes. We couple to the ring resonator at $l=1$ ($l=3$) with an extra ring resonator having a resonance at $\omega_{m=-4}$, ($\omega_{m=+4}$), and are off resonance at all other side-band frequencies. To excite the system, we inject into the additional resonator associated with the $l=1$ resonator with a pulse that has its carrier frequency $\omega_{m=-4}$ and the temporal full width at half-maximum (FWHM) $\Delta t=50\ n_0L/c$, corresponding to the FWHM of the spectral intensity $\Delta\omega=0.055\ c/n_0L\ll\Omega$. Therefore the input pulse only excites a single side band. The topologically protected one-way edge state converts the input at $\omega_{m=-4}$ to the frequency component at $\omega_{m=4}$ when the signal propagates along the edge of the lattice. We plot the input and output intensity spectra and the convert spectra in Fig. 4(b). The input field has a single frequency near $\omega_{m=-4}$ to excite the edge mode in the band gap. The output spectra are measured at detector 2 and we see that the field has been converted to the field with the frequency near $\omega_{m=4}$ with an efficiency of 81%. Our result shows that this system serves the purpose of a higher-order frequency converter.

Our proposal here can be implemented in various systems in fiber optics or integrated photonics. For the standard fiber system, the electro-optic phase modulation frequency can be up to ~1 GHz. This requires that the resonator be composed of the loop of a fiber with the length of ~0.1 m. We note that the standard single-mode fiber has a zero group velocity dispersion point at $\lambda=1.3$ μm, which is useful for our design here. For a silicon resonator modulated at ~100 GHz, the radius of the resonator is ~100 μm [25]. Flat and low intracavity dispersion over a wide wavelength range (~500 nm) can be achieved in a curving waveguide [26]. Further miniaturization of the structure in either platform can be accomplished with the use of slow-light waveguides.

In summary, we generalize the concept of photonic gauge potential to a synthetic space with both the spatial and frequency dimensions, and demonstrate that such a gauge potential leads to an edge state in the synthetic space that is useful for high-efficiency conversion to higher-order side bands. Related to and independent of our work, a recent preprint [27] has proposed the use of similar synthetic gauge potential for simulation of quantum hall effect in four dimensions. We believe that the concept of gauge potential in such synthetic space provides a new dimension for the control of light in both the real and the frequency spaces.

Funding. Air Force Office of Scientific Research (AFOSR) (FA9550-12-1-0488)

Acknowledgment. The authors acknowledge discussions with I. Carussotto, who alerted us to Ref. [27] when we were in the final stage of preparing this Letter.

REFERENCES

1. M. Hafezi, E. A. Demler, M. D. Lukin, and J. M. Taylor, Nat. Phys. **7**, 907 (2011).
2. R. O. Umucalilar and I. Carusotto, Phys. Rev. A **84**, 043804 (2011).
3. F. Liu and J. Li, Phys. Rev. Lett. **114**, 103902 (2015).
4. K. Fang and S. Fan, Phys. Rev. A **88**, 043847 (2013).
5. K. Fang, Z. Yu, and S. Fan, Nat. Photonics **6**, 782 (2012).
6. R. Fleury, A. B. Khanikaev, and A. Alù, "Floquet topological insulators for sound," arXiv:1511.08427 (2015).
7. M. Hafezi, S. Mittal, J. Fan, A. Migdall, and J. M. Taylor, Nat. Photonics **7**, 1001 (2013).
8. K. Fang and S. Fan, Phys. Rev. Lett. **111**, 203901 (2013).
9. Q. Lin and S. Fan, Phys. Rev. X **4**, 031031 (2014).
10. M. Onoda, S. Murakami, and N. Nagaosa, Phys. Rev. Lett. **93**, 083901 (2004).
11. S. Raghu and F. D. M. Haldane, Phys. Rev. A **78**, 033834 (2008).
12. F. D. M. Haldane and S. Raghu, Phys. Rev. Lett. **100**, 013904 (2008).
13. Z. Wang, Y. Chong, J. D. Joannopoulos, and M. Soljačić, Phys. Rev. Lett. **100**, 013905 (2008).
14. Z. Wang, Y. Chong, J. D. Joannopoulos, and M. Soljačić, Nature **461**, 772 (2009).
15. K. Fang, Z. Yu, and S. Fan, Phys. Rev. B **84**, 075477 (2011).
16. A. B. Khanikaev, S. H. Mousavi, W.-K. Tse, M. Kargarian, A. H. MacDonald, and G. Shvets, Nat. Mater. **12**, 233 (2013).
17. M. C. Rechstman, J. M. Zeuner, Y. Plotnik, Y. Lumer, D. Podolsky, F. Dreisow, S. Nolte, M. Segev, and A. Szameit, Nature **496**, 196 (2013).
18. S. Mittal, J. Fan, A. Faez, J. M. Taylor, and M. Hafezi, Phys. Rev. Lett. **113**, 087403 (2014).
19. L. Lu, J. D. Joannopoulos, and M. Soljačić, Nat. Photonics **8**, 821 (2014).
20. L. Yuan and S. Fan, Phys. Rev. A **92**, 053822 (2015).
21. A. Celi, P. Massignan, J. Ruseckas, N. Goldman, I. B. Spielman, G. Juzeliūnas, and M. Lewenstein, Phys. Rev. Lett. **112**, 043001 (2014).
22. X.-W. Luo, X. Zhou, C.-F. Li, J.-S. Xu, G.-C. Guo, and Z.-W. Zhou, Nat. Commun. **6**, 7704 (2014).
23. H. A. Haus, *Waves and Fields in Optoelectronics* (Prentice-Hall, 1984).
24. B. E. A. Saleh and M. C. Teich, *Fundamentals of Photonics* (Wiley, 1991).
25. L. D. Tzuang, M. Soltani, Y. H. D. Lee, and M. Lipson, Opt. Lett. **39**, 1799 (2014).
26. L. Zhang, Y. Yue, R. G. Beausoleil, and A. E. Willner, Opt. Express **19**, 8102 (2011).
27. T. Ozawa, H. M. Price, N. Goldman, O. Zilberberg, and I. Carusotto, "Synthetic dimensions in integrated photonics: From optical isolation to 4D quantum Hall physics," arXiv:1510.03910 (2015).